ERDC/GSL TR-08-16

Geotechnical and Structures Laboratory

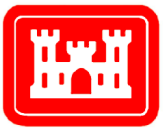

US Army Corps
of Engineers®
Engineer Research and
Development Center

Homogenization via Sequential Projections onto Nested Subspaces Spanned by Orthogonal Scaling and Wavelet Orthonormal Families of Functions

Luis A. de Béjar

July 2008

ERDC/GSL TR-08-16
July 2008

Homogenization via Sequential Projections onto Nested Subspaces Spanned by Orthogonal Scaling and Wavelet Orthonormal Families of Functions

Luis A. de Béjar

Geotechnical and Structures Laboratory
U.S. Army Engineer Research and Development Center
3909 Halls Ferry Road
Vicksburg, MS 39180-6199

Final report

Prepared for Headquarters, U.S. Army Corps of Engineers
Washington, DC 20314-1000

Abstract: This report presents a summary introduction to the homogenization procedure in numerical methods via sequential projections onto nested subspaces spanned by mutually orthogonal scaling and wavelet orthonormal families of functions. The ideas behind the technique of multi-resolution analysis unfold from the theory of linear operators in Hilbert spaces. The homogenization procedure through successive multi-resolution projections is presented, followed by a numerical example of sequential analysis and synthesis of a simple signal illustrating the application of the theory. A structural example shows a practical application of multi-resolution analysis to the displacement response of a cantilever with highly heterogeneous elasticity subjected to a concentrated load at the tip. An introductory appendix describes the reproducing kernel methods of mathematical representation of a given field.

Contents

Figures and Tables

Figures

Preface

The study reported herein was sponsored by Headquarters, U.S. Army Corps of Engineers, under the Military Engineering Research Program entitled “Multi-scale Modeling of the Structure of Materials for Adaptive Protection.” Dr. Reed L. Mosher, U.S. Army Engineer Research and Development Center (ERDC), was lead ERDC Technical Director for Military Engineering.

This investigation was conducted by personnel of the ERDC Geotechnical and Structures Laboratory (GSL), Vicksburg, MS, under the general supervision of Dr. David W. Pittman, Director, GSL; Dr. William P. Grogan, Deputy Director, GSL; Dr. Robert L. Hall, Chief, Geosciences and Structures Division (GSD); and Frank D. Dallriva, Chief, Structural Mechanics Branch (SMB). This report was prepared by Dr. Luis A. de Béjar, Research Structural Engineer, SMB, under the supervision of Dr. John F. Peters, Senior Research Scientist.

COL Richard B. Jenkins was Commander and Executive Director of ERDC. Dr. James R. Houston was Director.

1 Introduction

The objective of this report is to provide a summary introduction to the homogenization procedure in numerical methods via sequential projections onto nested subspaces spanned by mutually orthogonal scaling and wavelet orthonormal families of functions. The development is intended to be essentially self-contained. The mathematical (Greenberg 1978; Gilbert 2006) and signal processing (Strang and Nguyen 1995; Vetterli and Kovačević 1995) backgrounds are outlined in logical sequence avoiding statement and theorem demonstrations. The organization of the mathematical background is built after the work of Gilbert. Readers needing further expansions of the exposed material should consult the fundamental literature listed in the references.

The ideas behind multi-resolution analysis unfold from the theory of linear operators in Hilbert spaces (Davis 1975; Kolmogorov and Fomin 1975; Akhiezer and Glazman 1993; Zwillinger 1996). The homogenization procedure through successive multi-resolution projections is presented in Chapter 5 (Mehraeen and Chen 2004), followed by a numerical example of sequential analysis and synthesis of a simple signal illustrating the application of the theory (Wavelet extension of Mathcad 2000). Then, a structural example shows a practical application of multi-resolution analysis to the displacement response of a cantilever with highly heterogeneous elasticity subjected to a concentrated load at the tip. The report ends with a succinct introductory appendix describing the reproducing kernel methods of mathematical representation of a subject field under investigation (Liu and Chen 1995).

2 Mathematical Background

Energy

Let Z denote the set of integers: $Z = \{...,-2,-1,0,+1,+2,...\}$,

and R denote the collection of real numbers: $R = \{-\infty,+\infty\}$.

The energy of an analogue signal $f(\bullet)$ defined on $X = R$ is an average measure of its size given by the square of its norm:

$$E(f) = \left\| f(x) \right\|^2 = \int_{-\infty}^{+\infty} \left| f(x) \right|^2 dx \tag{1a}$$

in a one-dimensional space, or by

$$E(f) = \iint_D \left| f(x,y) \right|^2 dx\,dy \tag{1b}$$

when $f(\bullet,\bullet)$ is defined in a two-dimensional space $D = R^2$ (case of a static image).

Similarly, the energy of a digital signal a (i.e., a sequence) defined on $X = Z$ (or on $D = Z^2$ in the two-dimensional case) is given by

$$E(a) = \sum_{n=-\infty}^{+\infty} \left| a_n \right|^2 \tag{2a}$$

or by

$$E(a) = \sum_{m,n=-\infty}^{+\infty} \left| a_{mn} \right|^2 \tag{2b}$$

in one- and two-dimensional spaces, respectively.

Then, for a finite-energy function (or signal) one has $E(f)<\infty$ and, similarly, for a finite-energy sequence one has $E(a)<\infty$. In the analogue case, the set of all finite-energy functions (i.e., functions that are square-integrable) is

denoted by $L_2(X)$; whereas, in the digital case, the set of all finite-energy sequences (i.e., sequences that are square summable) is denoted by $\ell_2(Z)$.

Inner product spaces

The energy of individual elements of a function vector space can be conveniently calculated using the notion of inner product.

Definition. Let ν be a function vector space. An inner product on ν is a mapping that translates pairs of elements of the space into corresponding scalars, in such a way that

$$(f,f) \geq 0, \text{ and } (f,f) = 0 \quad \textit{iffi} \quad f = 0 \tag{3a}$$

$$(f,g) = \overline{(g,f)}, \tag{3b}$$

$$(f+g,h) = (f,h) + (g,h) \tag{3c}$$

$$(\lambda \cdot f, g) = \lambda \cdot (f,g) \Rightarrow (f, \lambda \cdot g) = \overline{(\lambda \cdot g, f)} = \overline{\lambda} \cdot (f,g) \tag{3d}$$

for all f, g, and h in ν, and where an over-lined variable means the complex conjugate of the variable. Spaces of finite-energy signals become inner-product spaces under the appropriate inner-product definition. For example, for the pair of analogue signals f, g in $L_2(X)$ one has

$$(f,g) = \int_{-\infty}^{+\infty} f(x) \cdot \overline{g(x)}\, dx \tag{4a}$$

and for the pair of sequences, $a = \{a_n\}_n$ and $b = \{b_n\}_n$ in $\ell_2(Z)$, one has

$$(a,b) = \sum_{n=-\infty}^{+\infty} a_n \cdot \overline{b_n} \tag{4b}$$

The three main properties of a complex inner product in ν are

Cauchy-Schwarz inequality:

$$\left|(f,g)\right|^2 \leq E(f) \cdot E(g) \tag{5a}$$

Triangle inequality:

$$E^{1/2}(f+g) \le E^{1/2}(f) + E^{1/2}(g) \tag{5b}$$

Polarization identity:

$$(f,g) = \frac{1}{4} \cdot \left\{ \left[E(f+g) - E(f-g) \right] + i \cdot \left[E(f+i \cdot g) - E(f-i \cdot g) \right] \right\} \tag{5c}$$

Orthonormal families

The inner product (f, g) of two functions gives a measure of how well f correlates with g. In fact, when f looks like g, then (f, g) will be close to the energy of g.

Definition. A subset $\{\varphi_n\}$ of an inner-product space ν is an orthonormal family when

$$\left(\varphi_i , \varphi_j \right) = \delta_{ij} \tag{6}$$

where δ_{ij} is Kronecker's delta, or, equivalently, when the family consists of mutually orthogonal elements, each having unit energy. For example, consider the family of sequences $\{\varepsilon^{(n)}\}_n$, with elements

$$\varepsilon^{(n)} = (\ldots 0,0,1,0,0,\ldots) \tag{7}$$

with unity at the n^{th} location, then

$$\left(\varepsilon^{(i)} , \varepsilon^{(j)} \right) = \delta_{ij} \tag{8}$$

and any sequence ($a = \{a_n\}_n$) $\in \ell_2(Z)$ may be represented as

$$a = \sum_n a_n \cdot \varepsilon^{(n)} = \sum_n \left(a, \varepsilon^{(n)} \right) \varepsilon^{(n)} \tag{9}$$

Definition. The expansion of a function f in an inner-product space ν in terms of the orthonormal family $\{\varphi_n\}$ in ν is defined by

$$S[f] = \sum_n (f, \varphi_n)\varphi_n \tag{10}$$

The numerical values (f, φ_n) are called the coefficients of f.

Notice that the family $\{\varphi_n\}$ is not necessarily complete, i.e., a basis spanning the space ν.

Bessel's inequality

Let $\{\varphi_n\}$ be an orthonormal family in an inner-product space ν. Then, the inequality

$$\sum_n \left|(f, \varphi_n)\right|^2 \le E(f) \tag{11}$$

holds for all f in ν. In other words, the sequence $\{ (f, \varphi_n) \}n$ of the coefficients of f has a finite energy that is bounded by $E(f)$ and, therefore, belongs to $\ell_2(Z)$.

Definition. An orthonormal family $\{\varphi_n\}$ in ν is complete when

$$\sum_n \left|(f, \varphi_n)\right|^2 = E(f) \tag{12}$$

for all f in ν.

Given a complete orthonormal family $\{\varphi_n\}$, then one can expand

$$S[f] = \sum_n (f, \varphi_n)\varphi_n = f \tag{13}$$

in the mean-square sense. In other words, the distance $D(f, S[f])$ tends to zero in the limit:

$$\lim E\left(f - \sum_{i=-N}^{N} (f, \varphi_i)\varphi_i \right) = 0, \quad as\, N \to \infty \tag{14}$$

Theorem. If $\{\varphi_n\}$is a complete orthonormal family in an inner-product space ν, then the coefficients (f,φ_n) satisfy the identities:

$$(Plancherel) \qquad E(f) = \sum_n \left| (f, \varphi_n) \right|^2 \tag{15a}$$

$$(Parseval) \qquad (f, g) = \sum_n (f, \varphi_n) \cdot \overline{(g, \varphi_n)} \tag{15b}$$

Fundamental bases

1. The simplest basis is the standard basis for $\ell_2(Z_N)$:

$$\varepsilon^{(n)} = (0,0,\ldots,0,1,0,\ldots,0,0), \qquad -\infty < n < +\infty \tag{16}$$

a complete orthogonal family whose n^{th} point carries the only non-zero component (unity) at the n^{th} location.

2. The Fourier basis for $\ell_2(Z_N)$:

$$\xi^{(k)} = \frac{1}{\sqrt{N}} \cdot \left(1, \omega^k, \omega^{2k}, \ldots, \omega^{k\cdot(N-1)}\right), \qquad k \geq 0 \tag{17}$$

where

$$\omega = e^{i\cdot\left(\frac{2\pi}{N}\right)} = cis\left(\frac{2\pi}{N}\right) \tag{18}$$

is an N^{th} root of unity, in the sense that $\omega^{k\cdot N} = 1$. Thus,

$$\xi^{(0)} = \frac{1}{\sqrt{N}} \cdot (1, 1, 1, \ldots, 1) \tag{19a}$$

$$\xi^{(1)} = \frac{1}{\sqrt{N}} \cdot \left(1, \omega, \omega^2, \ldots, \omega^{(N-1)}\right) \tag{19b}$$

$$\xi^{(N-1)} = \frac{1}{\sqrt{N}} \cdot \left(1, \omega^{N-1}, \omega^{2(N-1)}, \ldots, \omega^{(N-1)^2}\right) \tag{19c}$$

is a complete orthonormal family.

3. Defining the fundamental functions:

$$\varphi^{(n)} = \frac{1}{\sqrt{2}} \cdot \left(\varepsilon^{2n} + \varepsilon^{2n+1} \right) \quad and \quad \tilde{\varphi}^{(n)} = \frac{1}{\sqrt{2}} \cdot \left(\varepsilon^{2n} - \varepsilon^{2n+1} \right) \tag{20}$$

then each of the sets $\{\varphi^{(n)}\}$ and $\{\tilde{\varphi}^{(n)}\}$ is orthonormal in ℓ_2 and, together, the set $\{\varphi^{(n)}, \tilde{\varphi}^{(n)}\}$ is a complete orthonormal family in ℓ_2. Consequently, every point x in ℓ_2 admits the block expansion:

$$x = \sum_n \left(x, \varphi^{(n)} \right) \varphi^{(n)} + \sum_n \left(x, \tilde{\varphi}^{(n)} \right) \tilde{\varphi}^{(n)} \tag{21}$$

4. Since

$$\int_a^{a+1} cis(2\pi m\xi) \cdot \overline{cis(2\pi n\xi)}\, d\xi = \delta_{mn} \tag{22}$$

the family $\{ cis(2\pi n\xi);\ -\infty<n<+\infty \}$ of period one is orthonormal and complete for the space $L_2[a, a+1]$, for any choice of a.

5. Since

$$\int_{-\infty}^{+\infty} b_{0n}(x) \cdot \overline{b_{0n}(x)}\, dx = \delta_{mn} \tag{23}$$

the family $\{b_{0n}:-\infty<n<+n\}$, $b_{0n} = b(x-n)$ of all integer delays of the box function with scale zero is orthonormal in $L_2[-\infty,+\infty]$. However, the family is not complete. (Consider the expansion of a Haar function in terms of this family, for example.)

6. Similarly, the Haar family

$$h_{kn}(x) = 2^{k/2} \cdot h\left(2^k \cdot x - n \right), \qquad -\infty < n < +\infty \tag{24}$$

is orthonormal, but not complete, in $L_2[-\infty,+\infty]$, for each fixed resolution k. (Consider the expansion of a box function in terms of the family, for example.)

7. By allowing all possible resolutions and integer delays of the Haar function, one obtains a complete orthonormal family in $L_2[-\infty,+\infty]$, since

$$\left(h_{jm}, h_{kl}\right) = 2^{\frac{(j+k)}{2}} \cdot \int_{-\infty}^{+\infty} h\left(2^j \cdot x - m\right) \cdot h\left(2^k \cdot x - l\right) dx = \delta_{jk} \cdot \delta_{ml} \quad (25)$$

Every finite-energy function in $L_2[-\infty,+\infty]$ admits a series expansion:

$$f(x) = \sum_{k,l} \left(f, h_{kl}\right) h_{kl}(x) \quad (26)$$

Conservative mappings

A linear operator, $\Im: \nu \Rightarrow W$, from one inner-product space ν into a possibly different inner-product space W is conservative when the squared norm of every point in the space is preserved upon transformation. Conservative transformations also preserve inner products.

3 Signal Processing Background

Delay

The delay operator on ℓ_2 is defined as the mapping

$$\Psi: \quad \{x_n\}_n \Rightarrow \{x_{n-1}\}_n \tag{27}$$

which preserves energy, i.e.,

$$E(\Psi\, x) = \sum_n |\, x_{n-1}\,|^2 = \sum_n |\, x_n\,|^2 = E(x) \tag{28}$$

Convolution

The convolution operator, or filtering, between two sequences is defined by the sequence with elements

$$(h * x)_n = \sum_m h_m \cdot x_{(n-m)} = \sum_m h_{(n-m)} \cdot x_m \tag{29}$$

or, in operator terms, as

$$(h * x) = \sum_m h_m \cdot \Psi^m (x) \tag{30}$$

By the triangle inequality, one has

$$E^{1/2}(h * x) = E^{1/2}\left(\sum_m h_m \cdot \Psi^m (x) \right) \le \left\{ \sum_m |\, h_m\,| \right\} \cdot E^{1/2}(x) \tag{31}$$

which is bounded if $\left\{ \sum_m |\, h_m\,| \right\} = K$ (a real constant). Therefore, the convolution operation preserves energy when the coefficients of the sequence h are absolutely convergent.

To identify the adjoint of the operator h, we notice that

$$(h*x,y)=\sum_n\left(\sum_m h_{(n-m)}\cdot x_m\right)\cdot\overline{y_n}=\sum_m x_m\cdot\left(\overline{\sum_n\overline{h_{(n-m)}}\cdot y_n}\right)=\left(x,h^*\ast y\right) \quad (32)$$

i.e., the adjoint operator is given by the sequence $h^*=\left\{\overline{h_{-n}}\right\}_n$.

Discrete-Time Fourier Transform

The Discrete-Time Fourier Transform (DTFT) is defined by the pair of inner products:

$$X(\xi)=\left(x,e_\xi\right),\qquad \xi\in\left[-\frac{1}{2},\frac{1}{2}\right] \quad (33)$$

$$x_n=\int_{-1/2}^{1/2}X(\xi)\cdot e_\xi[n]\,d\xi \quad (34)$$

where $e_\xi = \{\, cis(2\pi n\xi)\,\}_n$. Notice that the transform $X(\xi)$, also called the frequency response function of x, has period one.

The DTFT (^) as a mapping from ℓ_2 into L_2[-1/2, +1/2] is energy preserving, and maps delay into modulation, i.e.,

$$\left(\Psi\, x\right)\hat{}\,(\xi)=\sum_n x_{n-1}\cdot e^{-2\pi i n\xi}=X(\xi)\cdot\overline{cis(2\pi\xi)} \quad (35)$$

A more crucial property of the DTFT is that it maps convolution into pointwise multiplication, i.e.,

$$(h*x)\hat{}\,(\xi)=\sum_n\left(\sum_m h_{n-m}\cdot x_m\right)\cdot\overline{cis(2\pi n\xi)}=H(\xi)\cdot X(\xi) \quad (36)$$

The frequency response function of the adjoint h^* is given by

$$\left(h^*\right)\hat{}\,(\xi)=\overline{\left\{\sum_n h_{-n}\cdot cis(2\pi n\xi)\right\}}=\overline{H(\xi)} \quad (37)$$

Since the transformation is conservative, inner products remain invariant upon transformation, i.e.,

$$\begin{aligned}(x,y) &= \int_{-1/2}^{1/2} X(\xi)\cdot\overline{Y(\xi)}\,d\xi = \sum_n \left(\int_{-1/2}^{1/2} X(\xi)\cdot cis(2\pi n\xi)\,d\xi \right)\cdot\overline{y_n} \\ &= \sum_n x_n\cdot\overline{y_n}\end{aligned} \tag{38}$$

for all finite-energy sequences in ℓ_2. Consequently, one has

$$x_n = \int_{-1/2}^{1/2} X(\xi)\cdot cis(2\pi n\xi)\,d\xi \tag{39}$$

z-Transform

The z-transform of a digital signal $x = \{x_n\}_n$ is defined as

$$X(z) = \sum_n x_n\cdot z^{-n}\,, \qquad z\in Complex \tag{40}$$

Since on the unit circle in the complex plane $z = z_o = \cdot cis\,(2\pi\xi)$, one can write

$$\hat{x}(\xi) = \left(x, e_\xi\right) = \sum_n x_n\cdot cis(-2\pi n\xi) = \sum_n x_n\cdot z_o^{-n} \tag{41}$$

and the z-transform can be regarded as the extension of the DTFT(x) from the unit circle to the whole complex plane.

Down-sampling

The down-sampling operation on a digital signal $x = \{x_n\}_n$ produces a new signal

$$(\downarrow 2)x = \{x_{2n}\}_n \tag{42}$$

by discarding all odd-indexed terms from x and re-indexing. Clearly, the down-sampling operation in not energy preserving, since

$$E\left((\downarrow 2)\,x\right) = \sum_n |x_{2n}|^2 \le \sum_n |x_n|^2 = E(x) \tag{43}$$

In Fourier transform terms one has

$$\frac{1}{2}\cdot\left\{ X\left(\frac{\xi}{2}\right)+X\left(\frac{\xi+1}{2}\right)\right\}=\frac{1}{2}\cdot\left\{ \sum_n x_n\cdot\overline{cis\left(n\cdot\pi\xi\right)}+\sum_n x_n\cdot\overline{cis\left(n\cdot\pi\left(\xi+1\right)\right)}+\right\}$$

$$=\frac{1}{2}\cdot\left\{ \sum_n x_n\cdot\overline{cis\left(n\cdot\pi\xi\right)}\cdot\left[1+\left(-1\right)^n\right]\right\} \tag{44}$$

$$=\left(\left(\downarrow 2\right)x,e_\xi\right)=\left[\left(\downarrow 2\right)x\right]\hat{}\left(\xi\right)$$

and, consequently, one obtains

$$\left[\left(\downarrow 2\right)x\right]\hat{}\left(\xi\right)=\frac{1}{2}\cdot\left\{X\left(\frac{\xi}{2}\right)+X\left(\frac{\xi+1}{2}\right)\right\} \tag{45}$$

which is an average in the frequency domain.

Up-sampling

By contrast, up-sampling is the converse of down-sampling. Given a digital signal $y = \{y_n\}_n$, up-sampling produces a new signal, defined by

$$\left(\uparrow 2\right)y=\left\{v_n\right\}_n,\quad such\ that\quad \left(v_{2n}\leftarrow y_n\right)and\left(v_{2n+1}\leftarrow 0\right) \tag{46}$$

Indeed, up-sampling is the adjoint operation to down-sampling, since

$$\left(\left(\downarrow 2\right)x,y\right)=\sum_n x_{2n}\cdot\overline{y_n}=\left(x,\left(\uparrow 2\right)y\right) \tag{47}$$

Up-sampling is a conservative operation and, in terms of the Fourier transform, one has

$$\left[\left(\uparrow 2\right)\hat{}\,y\right]\left(\xi\right)=\left(\left(\uparrow 2\right)y,e_\xi\right)=\left(y,e_{(2\xi)}\right)=Y\left(2\xi\right) \tag{48}$$

which is a ½-period function in the frequency domain.

Filters

A discrete filter is a linear, time-invariant operator Ξ acting on ℓ_2. In other words, the filtering operator Ξ satisfies the commutative property, i.e.,

$$\Xi(\Psi x) = \Psi(\Xi(x)) \tag{49}$$

with respect to the delay operator. Any such operator is given the following convolution:

$$h * x = \left\{ \sum_{\ell} h_{\ell} \cdot x_{n-\ell} \right\}_n \tag{50}$$

in which $h = \{h_n\}_n$ is the sequence of filter coefficients. Another way of expressing this crucial operation is

$$\Xi(x) = \sum_{\ell} h_{\ell} \cdot \Psi^{\ell}(x) \tag{51}$$

When only finitely many of the h_ℓ are different from zero, the operator Ξ is said to be of finite impulse response (FIR).

Since the DTFT maps convolution into point-wise multiplication, one has

$$y = \Xi(x) = h * x \qquad \Rightarrow \qquad Y(\xi) = H(\xi) \cdot X(\xi) \tag{52}$$

where $H(\xi) = (h, e_\xi)$ is the frequency response function of the filter coefficients. The effect of Ξ is to select or to reject certain frequencies in a signal. An FIR filter is said to "try hard" to be a low-pass filter when $H(0) \neq 0$ and $H(\pm 1/2) = 0$; by contrast, Ξ is said to "try hard" to be a high-pass filter when $H(0) = 0$ and $H(\pm 1/2) \neq 0$. Corresponding to every low-pass filter Ξ, there is an associate high-pass filter $\tilde{\Xi}$. Define $\tilde{\Xi}$ as the FIR filter having coefficients $\tilde{h}_n$, such that

$$\tilde{h}_n = (-1)^n \cdot \overline{h_{1-n}} \tag{53}$$

Then, by Fourier transforming to the frequency domain, one has

$$\overline{H}(\xi) = \overline{e_{\left(\xi+1/2\right)}} \cdot \overline{H}\left(\xi + 1/2\right) \tag{54}$$

Some fundamental filter examples are

1. Haar's filters, defined by

$$h_n = \begin{cases} 1/\sqrt{2}, & n = 0 \\ 1/\sqrt{2}, & n = 1 \\ 0, & n \neq 0,1 \end{cases} \tag{55a}$$

and

$$\tilde{h}_n = \begin{cases} 1/\sqrt{2}, & n = 0 \\ -1/\sqrt{2}, & n = 1 \\ 0, & n \neq 0,1 \end{cases} \tag{55b}$$

The corresponding frequency response functions are

$$H(\xi) = \sqrt{2} \cdot \overline{cis(\pi\xi)} \cdot \cos(\pi\xi) \tag{56a}$$

and

$$\tilde{H}(\xi) = \sqrt{2} \cdot i \cdot \overline{cis(\pi\xi)} \cdot \sin(\pi\xi). \tag{56b}$$

Clearly, $\tilde{H}(\xi)$ tries hard to be a high-pass filter having a single zero at the origin in the frequency domain.

2. The tent filters, defined by

$$g_n = \begin{cases} 1/2\cdot\sqrt{2}, & n = 0,2 \\ 1/\sqrt{2}, & n = 1 \\ 0, & otherwise \end{cases} \tag{51a}$$

and

$$\tilde{g}_n = \begin{cases} -1/2\cdot\sqrt{2}, & n=-1,1 \\ 1/\sqrt{2}, & n=0 \\ 0, & otherwise \end{cases} \tag{51b}$$

The corresponding frequency response functions are

$$G(\xi) = \sqrt{2}\cdot\overline{cis(2\pi\xi)}\cdot\cos^2(\pi\xi) \tag{58a}$$

and

$$\tilde{G}(\xi) = \sqrt{2}\cdot\sin^2(\pi\xi) \tag{58b}$$

Clearly, $\tilde{G}(\xi)$ tries hard to be a high-pass filter having a double zero at the origin in the frequency domain.

(3) Daubechies's db-2 filter, defined by the following only non-zero coefficients,

$$h_0 = \frac{1+\sqrt{3}}{4\sqrt{2}};\ h_1 = \frac{3+\sqrt{3}}{4\sqrt{2}};\ h_2 = \frac{3-\sqrt{3}}{4\sqrt{2}};\ and\ \ h_3 = \frac{1-\sqrt{3}}{4\sqrt{2}} \tag{59}$$

with corresponding frequency response function given by

$$H(\xi) = \sqrt{2}\cdot\overline{cis(3\pi\xi)}\cdot\cos^2(\pi\xi)\cdot\left[\cos(\pi\xi) + i\sqrt{3}\cdot\sin(\pi\xi)\right] \tag{60}$$

This filter has a double zero at $\xi = \pm 1/2$.

Filtering with sampling rate changes

Given an FIR filter Ξ, the following composite operators are defined consistently:

$$\left(\downarrow 2\circ\Xi^*\right): x \ \Rightarrow\ \left\{\sum_\ell x_\ell\cdot\overline{h_{\ell-2n}}\right\}_n \quad (for\ analysis) \tag{61a}$$

and

$$\left(\Xi \circ \uparrow 2\right) : x \;\Rightarrow\; \left\{ \sum_{\ell} x_{\ell} \cdot h_{n-2\ell} \right\}_{n} \quad (\textit{for synthesis}) \tag{61b}$$

where the superscript * means the adjoint operator. Notice that each composite operator in Equations 61a–b is the adjoint of its companion. Indeed, one has

$$\left(\Xi \circ \uparrow 2\right)^{*} = \left(\uparrow 2\right)^{*} \circ \Xi^{*} = \downarrow 2 \circ \Xi^{*} \tag{62}$$

Also notice that, in terms of the frequency response functions, one has

$$\left[\left(\downarrow 2 \circ \Xi^{*}\right) x\right]^{\wedge}(\xi) = \frac{1}{2} \cdot \left\{ \overline{H\left(\frac{\xi}{2}\right)} \cdot X\left(\frac{\xi}{2}\right) + \overline{H\left(\frac{\xi+1}{2}\right)} \cdot X\left(\frac{\xi+1}{2}\right) \right\} (\textit{for analysis}) \tag{63a}$$

and

$$\left[\left(\Xi \circ \uparrow 2\right) x\right]^{\wedge}(\xi) = H(\xi) \cdot X(2\xi) \tag{63b}$$

Consider (for simplicity) the Haar's filters and fix the sequences $a = \{a_n\}_n$ and $c = \{c_n\}_n$. Then, the fundamental sets of sequences $\{\varphi^{(n)}\}$ and $\{\tilde{\varphi}^{(n)}\}$ are given by

$$\varphi^{(n)} = \frac{1}{\sqrt{2}} \cdot \left(\varepsilon^{(2n)} + \varepsilon^{(2n+1)} \right) \tag{64}$$

and

$$\tilde{\varphi}^{(n)} = \frac{1}{\sqrt{2}} \cdot \left(\varepsilon^{(2n)} - \varepsilon^{(2n+1)} \right) \tag{65}$$

And, subsequently, one can compute for analysis the coefficients produced by the operations:

1. Averaging:

$$\left(\downarrow 2 \circ \Xi^{*}\right) a = \sum_{n} \frac{1}{\sqrt{2}} \cdot \left(a_{2n} + a_{2n+1}\right) \varepsilon^{(n)} = \left\{ \left(a, \varphi^{(n)}\right) \right\}_{n} \tag{66}$$

and

2. Differencing:

$$\left(\downarrow 2 \circ \tilde{\Xi}^{*}\right) a = \sum_{n} \frac{1}{\sqrt{2}} \cdot \left(a_{2n} - a_{2n+1}\right) \varepsilon^{(n)} = \left\{ \left(a, \tilde{\varphi}^{(n)}\right) \right\}_{n} \tag{67}$$

And, for synthesis, the orthogonal series expansions produced by the operations:

3. Spreading:

$$\left(\Xi \circ \uparrow 2\right)_{n} = \sum_{\ell} c_{\ell} \cdot h_{n-2\ell} = \begin{cases} \frac{1}{\sqrt{2}} \cdot c_{m} & , \ n=2m \\ \frac{1}{\sqrt{2}} \cdot c_{m} & , \ n=2m+1 \end{cases} \tag{68}$$

$$\left(\Xi \circ \uparrow 2\right) c = \sum_{n} c_{n} \cdot \varphi^{(n)} \tag{69}$$

and

4. Spreading and oscillating:

$$\sum_{\ell} c_{\ell} \cdot \tilde{h}_{n-2\ell} = \begin{cases} \frac{1}{\sqrt{2}} \cdot c_{m} & , \ n=2m \\ -\frac{1}{\sqrt{2}} \cdot c_{m} & , \ n=2m+1 \end{cases} \tag{70}$$

$$\left(\tilde{\Xi} \circ \uparrow 2\right) c = \sum_{n} c_{n} \cdot \tilde{\varphi}^{(n)} \tag{71}$$

Applying operation 1 followed by operation 3, one obtains the process (analysis + synthesis) for the coarse details in the digital signal a as

$$\left(\Xi \circ \uparrow 2\right) \circ \left(\downarrow 2 \circ \Xi^{*}\right) a = \sum_{n} \left(a, \varphi^{(n)}\right) \varphi^{(n)} \tag{72}$$

and, applying operation 2 followed by operation 4, one obtains the process (analysis + synthesis) for the fine details in the digital signal a as

$$\left(\tilde{\Xi} \circ \uparrow 2\right) \circ \left(\downarrow 2 \circ \tilde{\Xi}^{*}\right) a = \sum_{n} \left(a, \tilde{\varphi}^{(n)}\right) \tilde{\varphi}^{(n)} \tag{73}$$

But, together, the two sets in Equations 72 and 73 form a complete orthonormal family in the space ℓ_2. Therefore, the analytical expression for splitting the digital signal a in terms of coarse-detail and fine-detail components, respectively, may be written as

$$a = \sum_{n} \left(a, \varphi^{(n)}\right) \varphi^{(n)} + \sum_{n} \left(a, \tilde{\varphi}^{(n)}\right) \tilde{\varphi}^{(n)} \tag{74}$$

Consequently, the coarse details come out of a low-pass filter, while the fine details come out of the associated high-pass filter. The down-sampling operation in Equations 66 and 67 introduces aliasing. Subsequently, the up-sampling operation in Equations 68–69 and 70–71 eliminates that aliasing and, hence, allows the reconstruction of the original signal. This decomposition constitutes a fundamental filter bank (Figure 1). Other filter banks can be constructed on the basis of different filters and compound filters based on this fundamental arrangement.

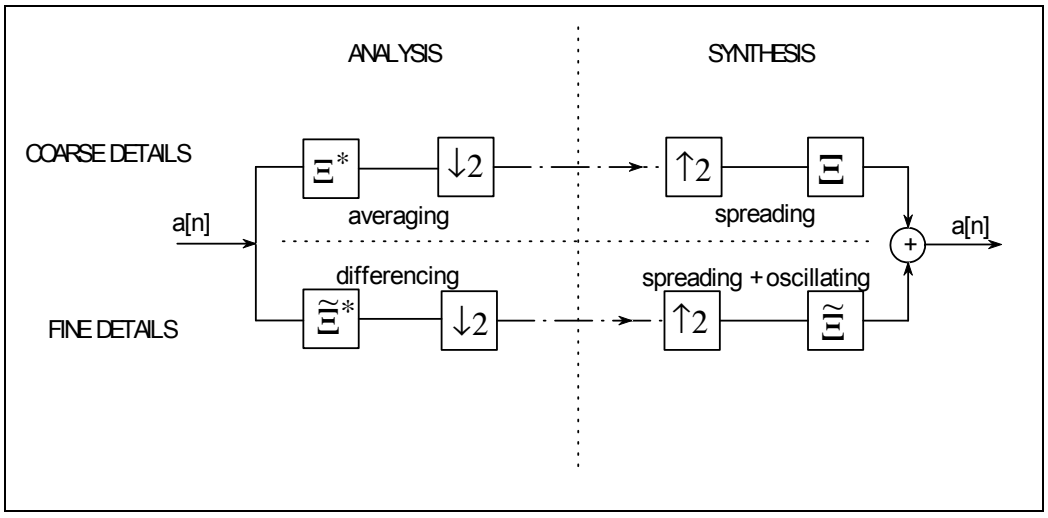

Figure 1. Fundamental filter bank.

Vetterli's conditions

Perfect reconstruction of the original digital signal can be achieved upon successive analysis followed by synthesis algorithms if the underlying filter satisfies the Vetterli's conditions stipulated as follows:

Let the vector $V(\xi)$ be defined as having two components. The first component is the frequency response function of the low-pass filter Ξ, $H(\xi)$, and the second component is the frequency response function of the associated high-pass filter. The Vetterli's conditions for the filter are

$$\left\| V(\xi) \right\|^2 = 2 \tag{75a}$$

in other words, the length of the vector $V(\xi) = \sqrt{2}$, and

$$\left(V(\xi), V\left(\xi + \tfrac{1}{2}\right) \right) = 0 \tag{75b}$$

in other words, $V(\xi)$ orthogonal to $V(\xi+1/2)$.

Scaling and wavelet functions

Given a filter defined by its coefficient sequence $h = \{h_m\}_m$, the fundamental definition of scaling function relates the function to itself at two contiguous levels of resolution by the expression

$$\varphi(x) = \sqrt{2} \cdot \left(\sum_m h_m \cdot \varphi(2x - m) \right) \tag{76}$$

in which the filter satisfies the condition

$$\sum_m h_m = \sqrt{2} \tag{77}$$

It can be shown that, through the satisfaction of the Vetterli's conditions, the set

$$\left\{ \varphi(x - n); \quad -\infty < n < +\infty \right\} \tag{78}$$

is an orthonormal family in the space $L_2(R)$.

Similarly, the fundamental definition of wavelet function relates the function to the associated scaling function at two contiguous levels of resolution by the expression

$$\psi(x) = \sqrt{2} \cdot \sum_m \tilde{h}_m \cdot \varphi(2x - m) \tag{79}$$

The mother wavelet $\psi(x)$ is *compactly supported* if the corresponding filter scaling function $\varphi(x)$ is *compactly supported*. In this case, it can also be shown that

$$\int_{-\infty}^{+\infty} \psi(x) \cdot \overline{\psi(x-s)} dx = (\downarrow 2)\left(\tilde{h} * \left(\tilde{h}\right)^*\right) = \varepsilon^{(0)} = \delta(s) \tag{80}$$

In other words, the set

$$\left\{\psi(\, x - n\,);\ \ -\infty < n < +\infty\right\} \tag{81}$$

is an orthonormal family in $L_2(R)$.

Again, by the same argument, one has

$$\left\{\int_{-\infty}^{+\infty} \varphi(x) \cdot \overline{\psi(x-s)}\, dx\right\}_{x \in Z} = (\downarrow 2)\left(h * \left(\tilde{h}\right)^*\right) = 0 \tag{82}$$

after Fourier transforming into the frequency domain, so that the family of scaling functions at a given level of resolution (different translations) and the family of associated wavelets at the same level of resolution (different translations) are mutually orthogonal to each other. Moreover, it can be shown that the system of child wavelets $\{\, 2^{k/2} \cdot \psi(\, 2^k x - n)\colon\ -\infty < k, n < +\infty\}$ [where k is the level of resolution, n is the translation, and the built-in amplitude $2^{k/2}$ is a normalization factor for unit energy] is a complete orthonormal family in $L_2(R)$. Therefore, this wavelet set constitutes a basis that spans the space of the finite-energy functions in $L_2(R)$.

4 Multi-Resolution Analysis

Let V_j be the closed subspace of $L_2(R)$ spanned by the scaling functions φ_{jk}, for a fixed integer j, where $\varphi_{jk}(x) = 2^{j/2} \cdot \varphi(2^j x - k)$. The sequence of subspaces $\{V_j\}_{j=-\infty}^{+\infty}$ defines a multi-resolution analysis with the following properties:

► The subspaces are nested:

$$\cdots \subset V_{-1} \subset V_0 \subset V_1 \subset \cdots \tag{83}$$

► The relations between coarse and fine scaling functions are determined by the following dilation and translation laws, respectively:

$$\varphi(x) \in V_j \quad \Rightarrow \quad \varphi(2x) \in V_{j+1}, \qquad j \in \mathrm{Z} \tag{84}$$

$$\varphi(x) \in V_0 \quad \Rightarrow \quad \varphi(x-n) \in V_0, \qquad n \in \mathrm{Z} \tag{85}$$

► The sequences of the V_j increase to all of $L_2(R)$ and decrease to the empty space.

► The set of integer translates $\{\varphi(x-k)\}_{k=-\infty}^{+\infty}$ is an orthonormal complete set, i.e., a basis for V_0.

The projection of $f(x)$ onto the subspace V_j is an approximation at the j^{th} level of resolution given by $f_j(x) = \sum_k c_{jk} \cdot \varphi_{jk}$, with the coefficient sequence c_{jk} given by the correlations

$$c_{jk} = \left(f, \varphi_{jk} \right) = \int_{-\infty}^{+\infty} f(x) \cdot \varphi_{jk}\, dx \tag{86}$$

The mother wavelet ψ may be derived from the father scaling function φ by the expression

$$\psi(x) = \sqrt{2} \cdot \sum_{k=0}^{N} \tilde{h}_k \cdot \varphi(2x-k), \quad where \quad \tilde{h}_k = (-1)^k \cdot \overline{h_{1-k}} \tag{87}$$

in which N is sufficiently large.

The orthogonal complement of V_j in V_{j+1} is given by the subspace W_j in such a way that

$$V_{j+1} = V_j \oplus W_j , \quad j \in \mathrm{Z} \tag{88}$$

where $\oplus$ is the direct sum between subspaces. Similarly to V_j, W_j is spanned by another orthonormal complete family (i.e., basis)

$$\psi_{jk}(x) = 2^{j/2} \cdot \psi\left(2^j x - k\right) \tag{89}$$

where $\psi(x)$ is the mother wavelet. This function is orthogonal to the fundamental scaling function with respect to translation:

$$\int_{-\infty}^{+\infty} \varphi(x) \cdot \overline{\psi(x-s)}\, dx = 0 \tag{90}$$

Based on the definition of scaling function, it follows that

$$V_j = V_i \oplus \left(\sum_{k=0}^{j-i-1} \oplus W_{i+k} \right), \quad j > i \tag{91}$$

Note that for a fixed j, the set $\{\varphi_{jk}\}$ spans the whole function space V_j and, therefore, any function can be approximated as the projection

$$P_j(f) = \sum_{k=-\infty}^{\infty} c_k \cdot \varphi_{jk} \tag{92}$$

where P_j is the projection operator onto the subspace V_j.

Figure 2 shows a conceptual view of the multi-resolution analysis procedure on a given digital signal.

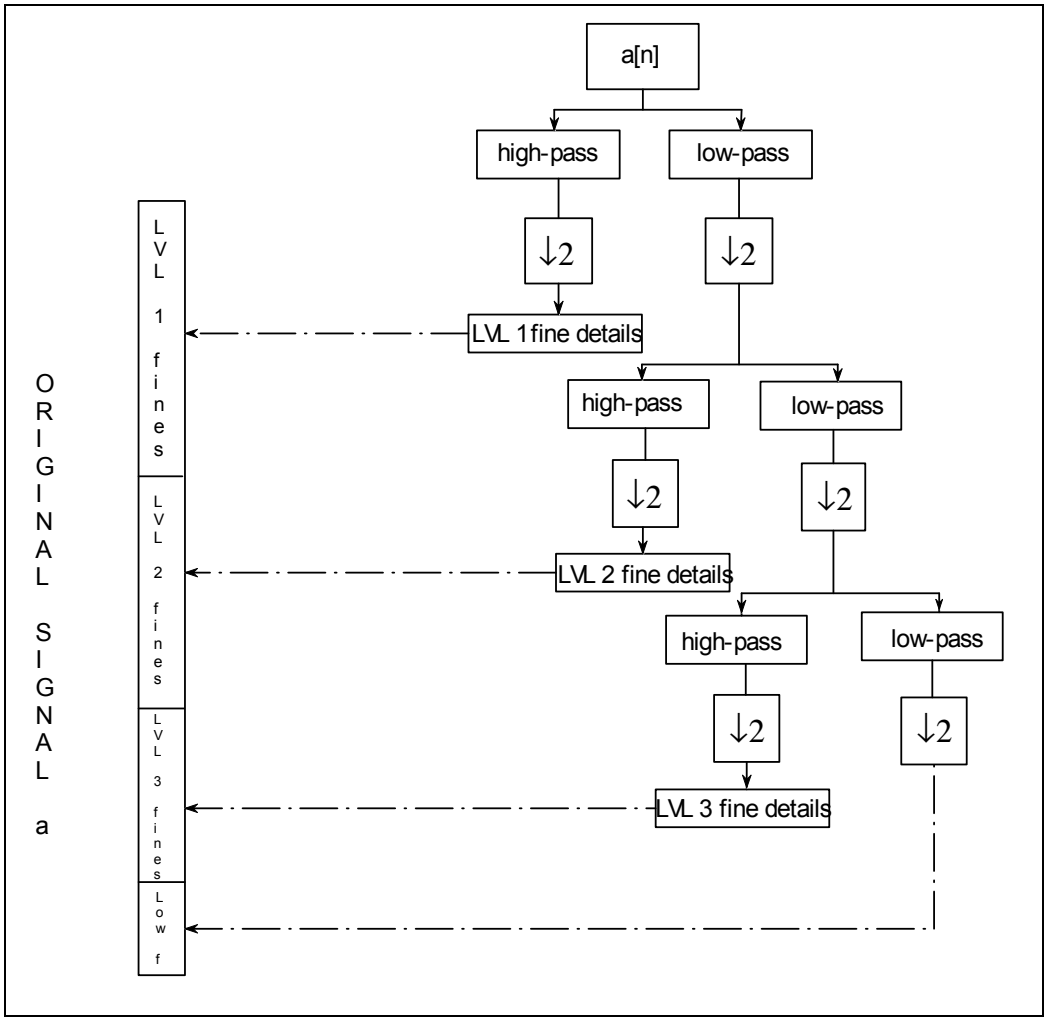

Figure 2. Conceptual multi-resolution analysis.

5 Homogenization via Projection Method

Let a discretized boundary value problem expressed in the function space V_{j+1} be

$$L_{j+1} \cdot U_{j+1} = F_{j+1} \tag{93}$$

in which the operator L_{j+1} acts on the space V_{j+1} spanned by the basis functions at the $(j+1)^{st}$ level of resolution. Consider the direct decomposition of the V_{j+1} space into the scaling-function and wavelet-function spaces:

$$V_{j+1} = V_j \oplus W_j \tag{94}$$

The fine and coarse components of V_{j+1} can be separated using discrete projecting operators as

$$w_j \cdot U_{j+1} = \begin{Bmatrix} U^h_{j+1} \\ U^\ell_{j+1} \end{Bmatrix} \tag{95}$$

where U_{j+1} is split into a coarse-detail component U^ℓ_{j+1} as a projection onto V_j, and a fine-detail component U^h_{j+1} as a projection onto W_j, and w_j is the wavelet transformation operator. In the case of the simple Haar basis, for example, the discrete form of the operator w_j is given by

$$w_j = \begin{Bmatrix} Q_j \\ P_j \end{Bmatrix} \tag{96}$$

where

$$P_j = \frac{1}{\sqrt{2}} \cdot \begin{bmatrix} 1 & 1 & 0 & 0 & . & . & 0 & 0 \\ 0 & 0 & 1 & 1 & . & . & 0 & 0 \\ . & . & . & . & . & . & . & . \\ 0 & 0 & 0 & 0 & . & . & 1 & 1 \end{bmatrix}_{\left(2^{j-1} x\, 2^j\right)} \tag{97a}$$

and

$$Q_j = \frac{1}{\sqrt{2}} \cdot \begin{bmatrix} 1 & -1 & 0 & 0 & . & . & 0 & 0 \\ 0 & 0 & 1 & -1 & . & . & 0 & 0 \\ . & . & . & . & . & . & . & . \\ 0 & 0 & 0 & 0 & . & . & 1 & -1 \end{bmatrix}_{\left(2^{j-1} x\, 2^j\right)} \tag{97b}$$

Recognizing that operator w_j is orthogonal, the transformation of Equation 93 renders

$$\begin{aligned} \left(w_j \cdot L_{j+1} \cdot w_j^T\right)\left(w_j \cdot U_{j+1}\right) &= \begin{bmatrix} L_{11} & L_{12} \\ L_{21} & L_{22} \end{bmatrix} \begin{Bmatrix} U_{j+1}^h \\ U_{j+1}^\ell \end{Bmatrix} \\ &= w_j \cdot F_{j+1} = \begin{Bmatrix} F_{j+1}^h \\ F_{j+1}^\ell \end{Bmatrix} \end{aligned} \tag{98}$$

where

$$\begin{Bmatrix} F_{j+1}^h \\ F_{j+1}^\ell \end{Bmatrix} = \begin{Bmatrix} Q_j \cdot F_{j+1} \\ P_j \cdot F_{j+1} \end{Bmatrix} \tag{99}$$

Applying static condensation, the reduced form of Equation 98 in terms of the coarse-detail component gives

$$\overline{L_{j+1}} \cdot U_{j+1}^\ell = F_{j+1}^\ell - L_{21} \cdot L_{11}^{-1} \cdot F_{j+1}^h \tag{100a}$$

where

$$\overline{L_{j+1}} = \left(L_{22} - L_{21} \cdot L_{11}^{-1} \cdot L_{12} \right)_{j+1} \tag{100b}$$

Then, the solution of Equation 100a may be decomposed into coarse- and fine-detail components before proceeding recursively to the next scale, i.e.,

$$\begin{Bmatrix} U_j^h \\ U_j^\ell \end{Bmatrix} = w_{j-1} \cdot U_{j+1}^\ell \tag{101}$$

The multi-scale homogenization procedure consists of generating and solving this sequence of homogenized equations followed by the corresponding decompositions.

6 Example of Signal Decomposition and Synthesis

Next, a numerical example of sequential analysis and synthesis of a simple signal is presented (MathSoft 2000). Figure 3 shows a bounded oscillatory signal with high-frequency components near the origin of time. Various multi-level fine details in the associated signal analysis are shown in Figure 4. The coarse components appear near the bottom of the figure, and the fine details are shown at increasing level of resolution as the reader moves up within the figure. The reconstructed original signal appears near the upper horizontal margin of the figure. The corresponding sequential reconstruction process is shown in Figure 5. Notice how the progressive addition of details eventually recovers the whole signal. The resultant signal at some intermediate level of resolution may be considered by the analyst as sufficient for practical applications, thereby economizing representation and calculation efforts.

The sequential exercise of decomposition and reconstruction is repeated in Figures 6–8 for the same signal, but with superimposed Gaussian noise. Note that the highest-resolution details are essentially pure random noise.

EXAMPLE 1. MULTI-RESOLUTION ANALYSIS:

$Trun := 1.024$ $\Delta T := 0.001$ $thisWave := coiflet(12)$

$N := \frac{Trun}{\Delta T}$ $i := 0..N-1$ $x_i := \Delta T \cdot i$ $N = 1.024 \cdot 10^3$

$doppler(x) := \sqrt{x \cdot (1-x)} \cdot \sin\left(2.1 \cdot \frac{\pi}{x + 0.05}\right)$

$y_i := doppler\left(\frac{x_i}{Trun}\right)$

$MaxDWTLevel(y) = 10$ $J := 6$ $j := 0..J-1$

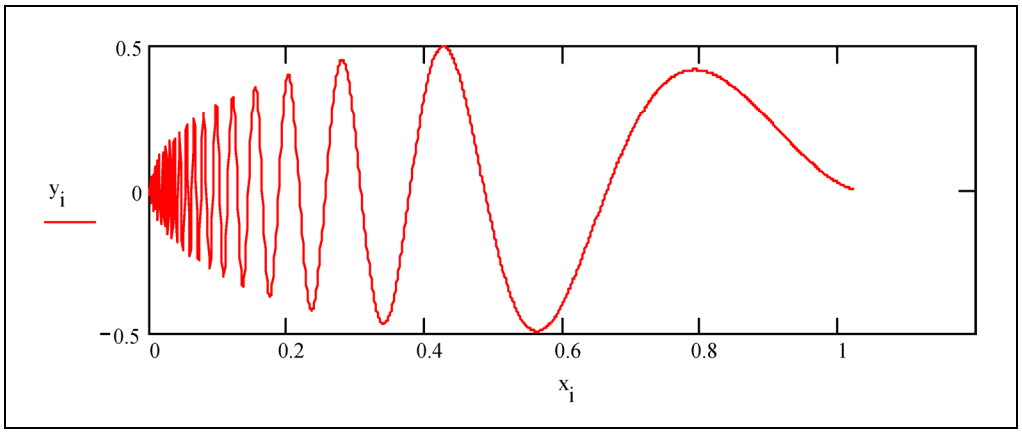

Figure 3. Signal with initial high-frequency oscillations.

Reference:E:\Program Files\MathSoft\Mathcad 8 Professional\HANDBOOK\wavelets\Mra1.mcd

$mra(v, J, filter) :=$
- $w \leftarrow dwt(v, J, filter)$
- $Z_{rows(v)-1} \leftarrow 0$
- $M^{<0>} \leftarrow idwt(put\_smooth(Z, J, get\_smooth(w, J)), J, filter)$
- for $qj \in J..1$
  - $Z_{rows(v)-1} \leftarrow 0$
  - $M^{<J+1-qj>} \leftarrow idwt(put\_detail(Z, qj, get\_detail(w, qj)), J, filter)$
- M^T

$M := mra(y, J, thisWave)$

$S6_i := M_{0,i}$

$D6_i := M_{1,i}$ $D5_i := M_{2,i}$ $D4_i := M_{3,i}$

$D3_i := M_{4,i}$ $D2_i := M_{5,i}$ $D1_i := M_{6,i}$

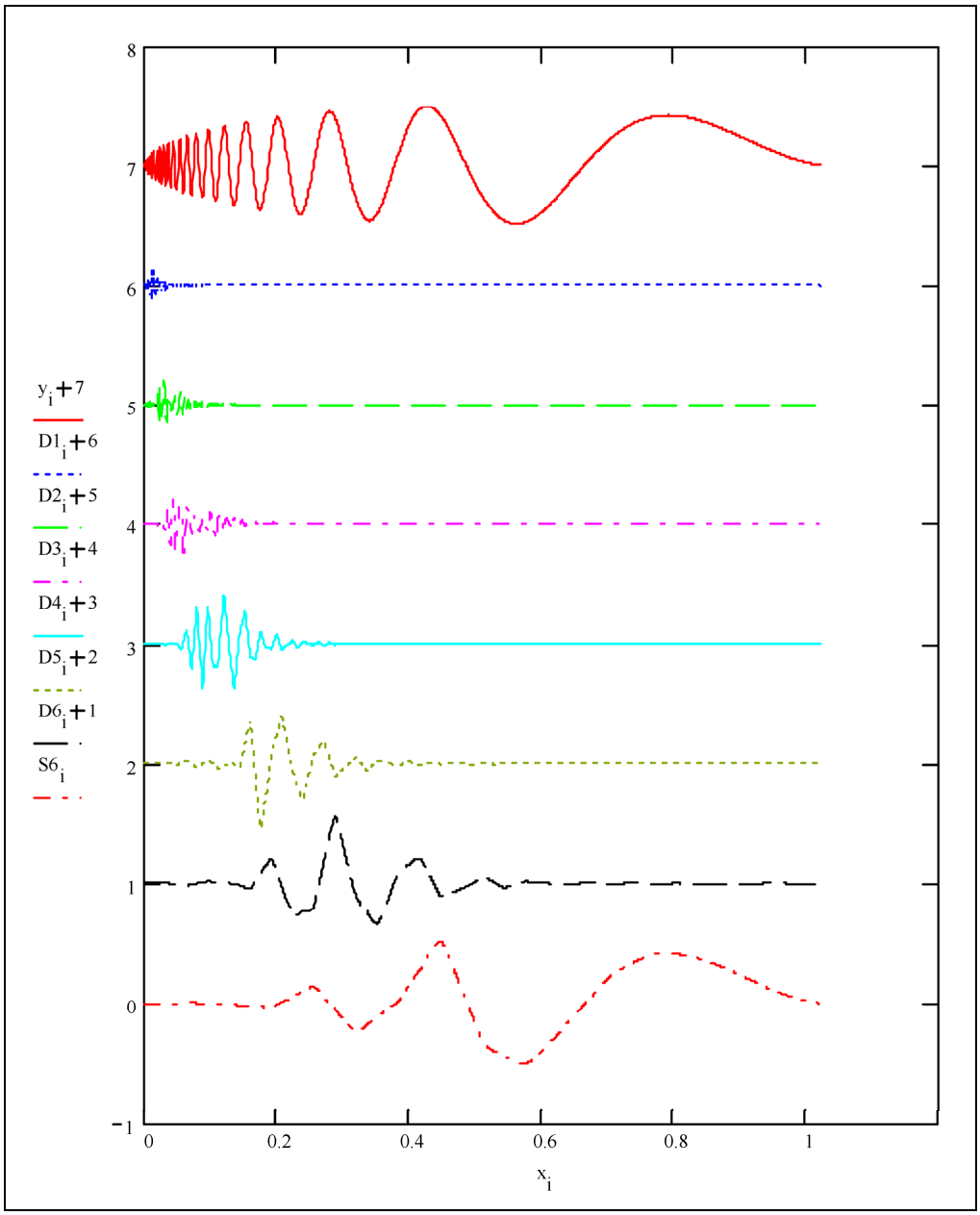

Figure 4. Multi-level fine details in signal analysis. (Resolution decreases from the top to the bottom of the figure.)

$$pf := 1$$

$$\text{mrapprox}(y, J, \text{filter}) := \left| \begin{array}{l} Q \leftarrow \text{mra}(y, J, \text{filter}) \\ \text{for } i \in 0..\text{rows}(y) - 1 \\ \quad \left| \begin{array}{l} M_{0,i} \leftarrow Q_{0,i} \\ \text{for } j \in 1..J \\ \quad M_{j,i} \leftarrow M_{j-1,i} + Q_{j,i} \end{array} \right. \\ M \end{array} \right.$$

$$MR := \text{mrapprox}(y, J, \text{thisWave})$$

$$S6_i := MR_{0,i} \qquad S5_i := MR_{1,i} \qquad S4_i := MR_{2,i} \qquad S3_i := MR_{3,i}$$

$$S2_i := MR_{4,i} \qquad S1_i := MR_{5,i} \qquad S0_i := MR_{6,i}$$

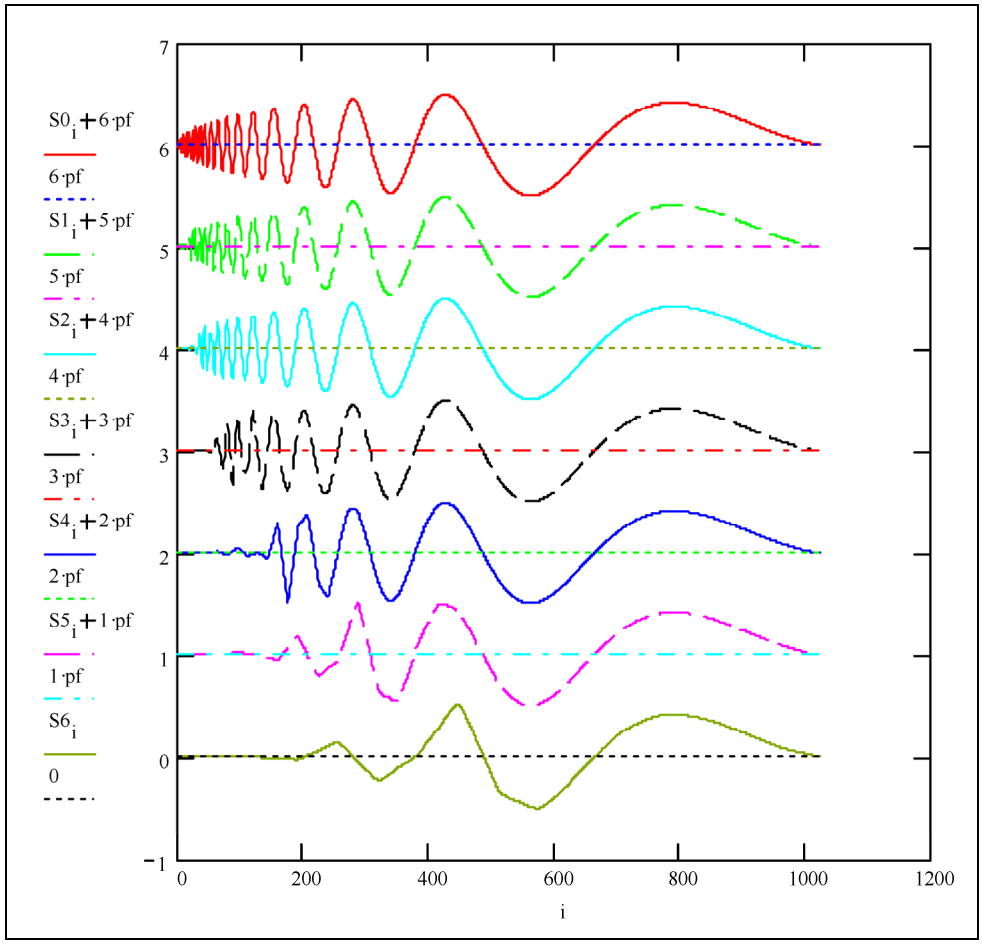

Figure 5. Reconstruction of original signal in multi-level synthesis process by progressive increase of resolution through the addition of fine details, starting by the coarsest representation at the bottom of the figure.

$\sigma := 0.1$ $\quad$ $noisy\_doppler := y + rnorm(rows(y), 0, \sigma)$

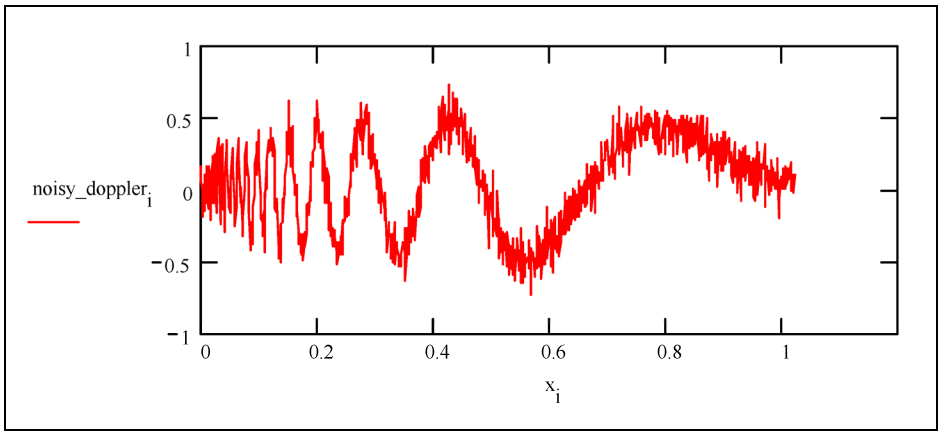

Figure 6. Noisy signal with initial high-frequency oscillations.

$MN := mra(noisy\_doppler, J, thisWave)$ $\quad$ $nd := noisy\_doppler$

$S6_i := MN_{0,i}$

$D6_i := MN_{1,i}$ $\quad$ $D5_i := MN_{2,i}$ $\quad$ $D4_i := MN_{3,i}$

$D3_i := MN_{4,i}$ $\quad$ $D2_i := MN_{5,i}$ $\quad$ $D1_i := MN_{6,i}$

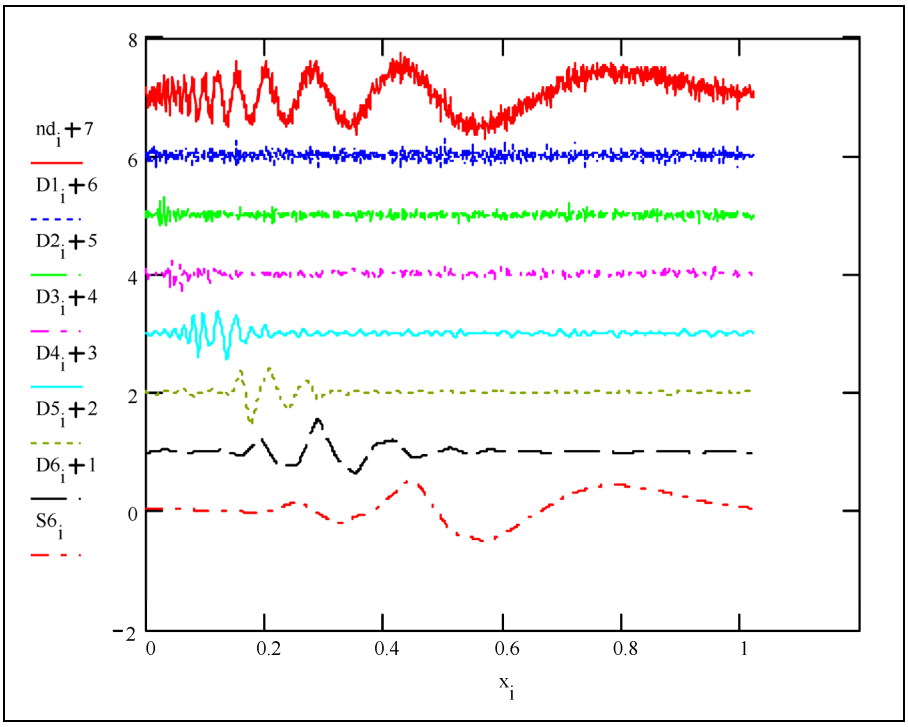

Figure 7. Multi-level fine details in signal analysis. (Resolution decreases from the top to the bottom of the figure.)

$$MRN := mrapprox(noisy\_doppler, J, thisWave)$$

$$S6_i := MRN_{0,i} \qquad S5_i := MRN_{1,i} \qquad S4_i := MRN_{2,i} \qquad S3_i := MRN_{3,i}$$

$$S2_i := MRN_{4,i} \qquad S1_i := MRN_{5,i} \qquad S0_i := MRN_{6,i}$$

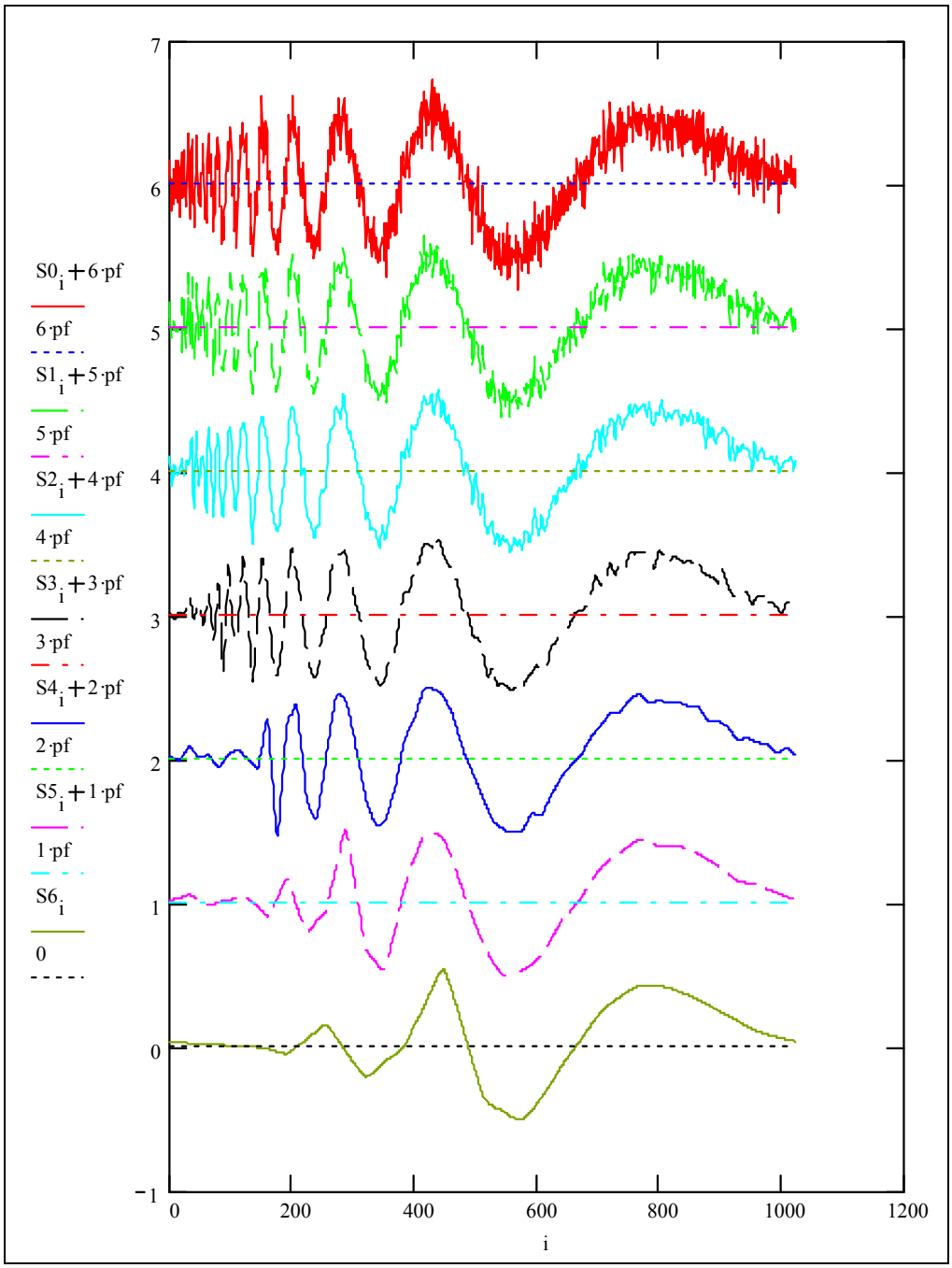

Figure 8. Reconstruction of original signal in multi-level synthesis process by progressive increase of resolution through the addition of fine details, starting by the coarsest representation at the bottom of the figure.

7 Simple Cantilever with Heterogeneous Harmonic Elasticity

In a practical application, a simple cantilever is subjected to a concentrated load at the tip. The cross section of the cantilever is uniform along its length, but the material elasticity is highly heterogeneous. In fact, Young's modulus of elasticity is modeled as a constant mean value plus a harmonic fluctuation about the mean whose frequency is a controlled parameter.

The exact static displacement response of the cantilever was obtained through the application of the virtual work principle and appears represented in Figure 9. Figure 10 shows the multi-level fine-detail decomposition with the coarsest component represented toward the bottom of the figure. The reconstructed original signal appears near the upper horizontal margin of the figure. The corresponding sequential reconstruction process is shown in Figure 11. Notice how the progressive addition of details eventually recovers the whole signal. However, in this case, interestingly, all levels of detail resolution have a significant contribution to the signal synthesis, particularly at the boundary ends, where both the essential boundary conditions (displacement of the cantilever tip at the right end) and the natural boundary conditions (reactive shear force and bending moment enforcing the zero displacement and slope at the support) are fundamental for the reconstruction at all stages of resolution. This is also true even when only the coarsest component of displacement response is considered.

EXAMPLE 2. HETEROGENEOUS CANTILEVER

>>> Define INPUT variables:

$alpha := 0.95$ Elastic modulus ratio Eo/Ea

*** CAREFUL: alpha=1 INSTABILITY ***

$n := 20$ Elastic modulus wave-number parameter

$dlambda := \frac{1}{128}$ Increment of response location parameter

$thisWave := coiflet(12)$

>>> Compute RESPONSE along cantilever:

$nsubs := 127$

$i := 0 .. nsubs$

$\lambda_i := i \cdot dlambda$ Response location parameter

$$mu0_i := \int_0^{\lambda_i} \frac{1}{1 + alpha \cdot \cos(2 \cdot \pi \cdot n \cdot \xi)} d\xi$$ M-matrix

$$mu1_i := \int_0^{\lambda_i} \frac{\xi}{1 + alpha \cdot \cos(2 \cdot \pi \cdot n \cdot \xi)} d\xi$$

$$mu2_i := \int_0^{\lambda_i} \frac{\xi^2}{1 + alpha \cdot \cos(2 \cdot \pi \cdot n \cdot \xi)} d\xi$$

$$\delta_i := \lambda_i \cdot mu0_i - \left(1 + \lambda_i\right) \cdot mu1_i + mu2_i$$

MaxDWTLevel(δ) = 10 J := 6 j := 0.. J – 1

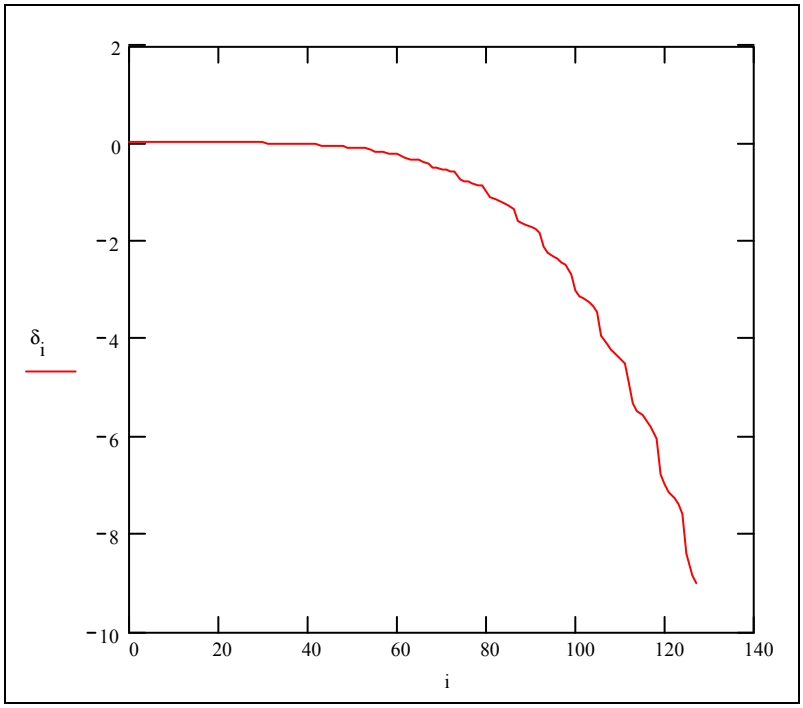

Figure 9. Exact displacement response of cantilever.

Reference:E:\Program Files\MathSoft\Mathcad 8 Professional\HANDBOOK\wavelets\Mra1.mcd

$$\begin{aligned}
&\text{mra}(v, J, \text{filter}) := \\
&\quad w \leftarrow \text{dwt}(v, J, \text{filter}) \\
&\quad Z_{\text{rows}(v)-1} \leftarrow 0 \\
&\quad M^{\langle 0 \rangle} \leftarrow \text{idwt}(\text{put_smooth}(Z, J, \text{get_smooth}(w, J)), J, \text{filter}) \\
&\quad \text{for } qj \in J .. 1 \\
&\qquad Z_{\text{rows}(v)-1} \leftarrow 0 \\
&\qquad M^{\langle J+1-qj \rangle} \leftarrow \text{idwt}(\text{put_detail}(Z, qj, \text{get_detail}(w, qj)), J, \text{filter}) \\
&\quad M^{T}
\end{aligned}$$

M := mra(δ, J, thisWave)

$$S6 := \left(M^{T}\right)^{<0>} \qquad D6 := \left(M^{T}\right)^{<1>} \qquad D5 := \left(M^{T}\right)^{<2>} \qquad D4 := \left(M^{T}\right)^{<3>}$$

$$D3 := \left(M^{T}\right)^{<4>} \qquad D2 := \left(M^{T}\right)^{<5>} \qquad D1 := \left(M^{T}\right)^{<6>}$$

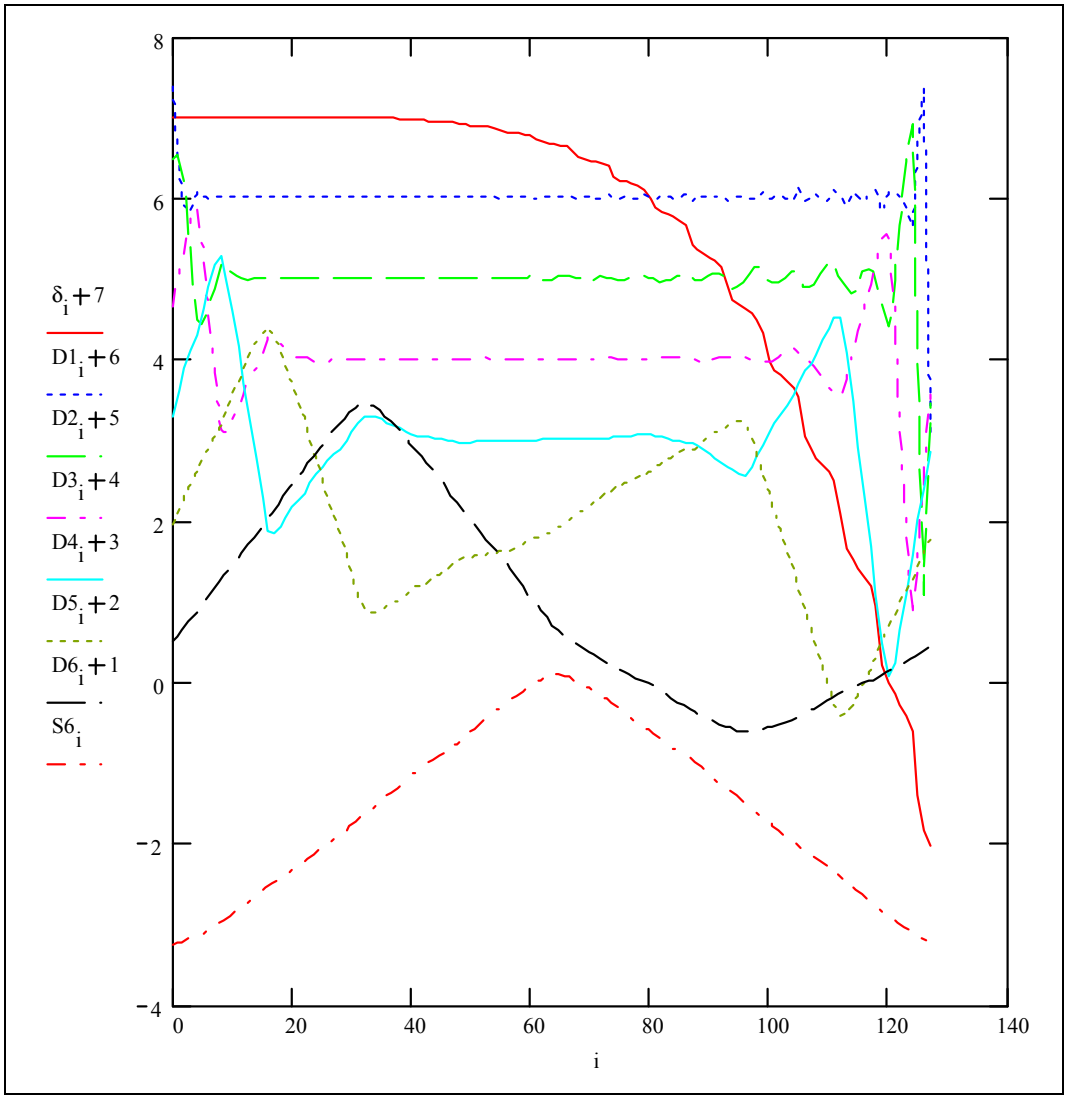

Figure 10. Multi-level fine details in displacement-response analysis. (Resolution decreases from the top to the bottom of the figure.)

$pf := 1$

$$mrapprox(y, J, filter) := \left| \begin{array}{l} Q \leftarrow mra(y, J, filter) \\ \text{for } i \in 0..rows(y) - 1 \\ \quad \left| \begin{array}{l} M_{0,i} \leftarrow Q_{0,i} \\ \text{for } j \in 1..J \\ \quad M_{j,i} \leftarrow M_{j-1,i} + Q_{j,i} \end{array} \right. \\ M \end{array} \right.$$

$MR := mrapprox(\delta, J, thisWave)$

$S6 := \left(MR^T\right)^{<0>}$ $S5 := \left(MR^T\right)^{<1>}$ $S4 := \left(MR^T\right)^{<2>}$ $S3 := \left(MR^T\right)^{<3>}$

$S2 := \left(MR^T\right)^{<4>}$ $S1 := \left(MR^T\right)^{<5>}$ $S0 := \left(MR^T\right)^{<6>}$

$i := 0 .. nsubs$

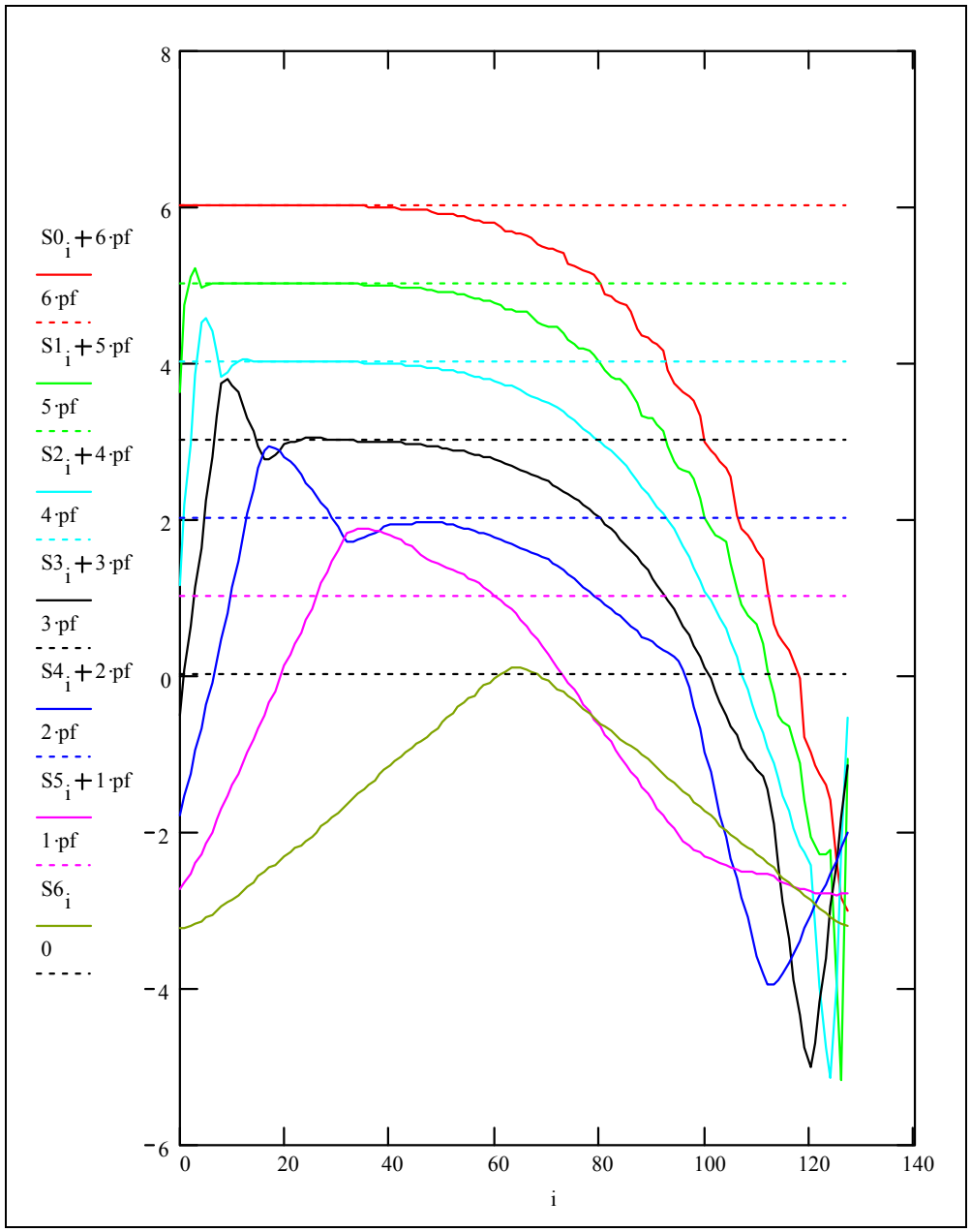

Figure 11. Reconstruction of exact displacement response in multi-level synthesis process by progressive increase of resolution through the addition of fine details, starting by the coarsest representation at the bottom of the figure.

References

Akhiezer, N. I., and I. M. Glazman. 1993. *Theory of linear operators in Hilbert space*. New York: Dover.

Davis, P. J. 1975. *Interpolation and approximation*. New York: Dover.

Gilbert, J. E. 2006. Wavelets and signal processing. Austin, TX: Department of Mathematics, Univ. of Texas.

Greenberg, M. D. 1978. *Foundations of applied mathematics*. Englewood Cliffs, NJ: Prentice-Hall.

Kolmogorov, A. N., and S. V. Fomin. 1975. *Introductory real analysis*. New York: Dover.

Liu, W. K., and Y. Chen. 1995. Wavelet and multiple scale reproducing kernel methods. *International Journal for Numerical Methods in Fluids* 21:901–931.

MathSoft. 2000. *Mathcad: User's guide*. Cambridge, MA.

Mehraeen, S., and J.-S. Chen. 2004. Wavelet-based multi-scale projection method in homogenization of heterogeneous media. *Finite Elements in Analysis and Design* 40:1665–1679.

Strang, G., and T. Nguyen. 1995. *Wavelets and filter banks*. Cambridge, MA: Wellesley-Cambridge Press.

Vetterli, M., and J. Kovačević. 1995. Wavelets and subband coding. Englewood Cliffs, NJ: Prentice-Hall.

Zwillinger, D. 1996. *Standard mathematical tables and formulae*. 30th ed. Boca Raton, FL: CRC Press.

Appendix A: Summary of Reproducing Kernel Representation

A uni-dimensional field $u(x)$ may be expressed as (Liu and Chen 1995)

$$u(x) = u^w(x) + \int_v <1\ x>[M]^{-1}\begin{Bmatrix}1\\ y\end{Bmatrix} u(y)\,\varphi\left(\frac{x-y}{a_0}\right)dy - \int_v <1\ x>[M]^{-1}\begin{Bmatrix}1\\ y\end{Bmatrix} u^w(y)\,\varphi\left(\frac{x-y}{a_0}\right)dy \tag{A1}$$

where u^w is the part of the field that may be obtained by multi-resolution wavelet reconstruction, $\varphi(\cdot)$ is the father scaling function, a_0 is the dilation parameter, and the window moment matrix $[M]$ is given by

$$[M] = \begin{bmatrix} m_0 & m_1 \\ m_1 & m_{11}\end{bmatrix} = \begin{bmatrix} \int_v \varphi\left(\frac{x-y}{a_0}\right)dy & \int_v y\cdot\varphi\left(\frac{x-y}{a_0}\right)dy \\ \int_v y\cdot\varphi\left(\frac{x-y}{a_0}\right)dy & \int_v y^2\cdot\varphi\left(\frac{x-y}{a_0}\right)dy\end{bmatrix} \tag{A2}$$

The factor $<1\ x>[M]^{-1}\begin{Bmatrix}1\\ y\end{Bmatrix}$ inside the integrals in Equation A1 may be expanded in terms of a correction function $C(x, y, a_0)$, given by

$$C(x,y,a_0) = C_1(x) + C_2(x)\cdot\left(\frac{x-y}{a_0}\right) \tag{A3a}$$

where

$$C_1(x) = -\frac{1}{a_0}\cdot\frac{m_{11}}{\Delta} \tag{A3b}$$

$$C_2(x) = -\frac{1}{a_0}\cdot\frac{m_1}{\Delta} \tag{A3c}$$

and $\Delta = \det(M)$.

Expanding the function $u^w(x)$ in the wavelet subspaces, one obtains the truncated-series approximation:

$$u^w(x) = \sum_{m=0}^{\infty} \sum_{n=n_1}^{n_2} (u, \psi_{mn})\, \psi_{mn}(x) \tag{A4}$$

where wavelet child $\psi_{mn}(x)$ corresponds to resolution m and translate n. Substituting Equations A3a and A4 into Equation A1, one gets the expression

$$\begin{aligned} u(x) = & \int_v C(x, y a_0) \cdot \varphi\left(\frac{x-y}{a_0}\right) \cdot u(y)\, dy \\ & + \sum_{m=0}^{\infty} \sum_{n=n_1}^{n_2} \left(\int_v u(y) \cdot \psi_{mn}(y)\, dy \right) \cdot \left[\psi_{mn}(x) - \tilde{\psi}_{mn}(x) \right] \end{aligned} \tag{A5}$$

where the functions $\tilde{\psi}_{mn}(x)$ are the approximations of the wavelet functions $\psi_{mn}(x)$ obtained from the reproducing kernel reconstruction. In fact, the first term in Equation A5 defines the reproducing kernel approximation (low-frequency components), whereas the second term in that equation gives the contribution of the high-frequency components. [For the low-frequency components, $\tilde{\psi}_{mn}(x) \sim \psi_{mn}(x)$.]

REPORT DOCUMENTATION PAGE

Form Approved
OMB No. 0704-0188

1. REPORT DATE *(DD-MM-YYYY)*	2. REPORT TYPE	3. DATES COVERED *(From - To)*
July 2008	Final report	

4. TITLE AND SUBTITLE

Homogenization via Sequential Projections onto Nested Subspaces Spanned by Orthogonal Scaling and Wavelet Orthonormal Families of Functions

5a. CONTRACT NUMBER

5b. GRANT NUMBER

5c. PROGRAM ELEMENT NUMBER

6. AUTHOR(S)

Luis A. de Béjar

5d. PROJECT NUMBER

5e. TASK NUMBER

5f. WORK UNIT NUMBER

7. PERFORMING ORGANIZATION NAME(S) AND ADDRESS(ES)

U.S. Army Engineer Research and Development Center
Geotechnical and Structures Laboratory
3909 Halls Ferry Road
Vicksburg, MS 39180-6199

8. PERFORMING ORGANIZATION REPORT NUMBER

ERDC/GSL TR-08-16

9. SPONSORING / MONITORING AGENCY NAME(S) AND ADDRESS(ES)

Headquarters, U.S. Army Corps of Engineers
Washington, DC 20314-1000

10. SPONSOR/MONITOR'S ACRONYM(S)

11. SPONSOR/MONITOR'S REPORT NUMBER(S)

12. DISTRIBUTION / AVAILABILITY STATEMENT

Approved for public release; distribution is unlimited.

13. SUPPLEMENTARY NOTES

14. ABSTRACT

This report presents a summary introduction to the homogenization procedure in numerical methods via sequential projections onto nested subspaces spanned by mutually orthogonal scaling and wavelet orthonormal families of functions. The ideas behind the technique of multi-resolution analysis unfold from the theory of linear operators in Hilbert spaces. The homogenization procedure through successive multi-resolution projections is presented, followed by a numerical example of sequential analysis and synthesis of a simple signal illustrating the application of the theory. A structural example shows a practical application of multi-resolution analysis to the displacement response of a cantilever with highly heterogeneous elasticity subjected to a concentrated load at the tip. An introductory appendix describes the reproducing kernel methods of mathematical representation of a given field.

15. SUBJECT TERMS

Hilbert spaces
Multi-resolution analysis
Nested subspace projections
Numerical homogenization
Reproducing kernel techniques
Signal processing
Wavelet and scaling functions

16. SECURITY CLASSIFICATION OF:			17. LIMITATION OF ABSTRACT	18. NUMBER OF PAGES	19a. NAME OF RESPONSIBLE PERSON
a. REPORT	b. ABSTRACT	c. THIS PAGE			19b. TELEPHONE NUMBER *(include area code)*
UNCLASSIFIED	UNCLASSIFIED	UNCLASSIFIED		47	